MODELING OF LEVEE EROSION UNDER IRREGULAR WAVES

Nobuhisa Kobayashi[1] and Heather Weitzner[2]

A levee erosion model is developed to predict the temporal and cross-shore variations of vertical erosion depth under irregular wave action. The product of the erosion rate and the turf resistance force is related to the wave energy dissipation rates due to wave breaking and bottom friction. The turf resistance force is expressed using the turf thickness and the surface and underneath resistance parameters. The empirical parameters are calibrated using available data. The calibrated model has been shown to reproduce the relation between the limiting velocity and steady flow duration, the erosion rate on a seaward grassed slope, and the eroded profile evolution of a seaward clay slope. The levee erosion model is also compared with field tests for erosion on the landward slope caused by wave overtopping. It is found to be difficult to reproduce the observed erosion initiation and progression because of the wide variations of the grass cover and clay resistance. The turf resistance parameters will need to be calibrated for specific levees.

Keywords: Levee; Dike; Erosion; Grass; Clay; Breaking Waves

INTRODUCTION

Levees (dikes) have been constructed to protect some coastal areas against flooding by the combined action of storm surge and wind waves. A number of large-scale laboratory experiments were conducted to quantify the resilience of seaward levee slopes (e.g., Klein Breteler et al. 2012). Erosion of landward levee slopes has been investigated on actual levees using the Wave Overtopping Simulator (e.g., van der Meer et al. 2010) which mimics irregular wave overtopping events for the specified wave overtopping rate. The separate studies for the seaward and landward levee slopes have not been synthesized probably because of the different hydrodynamics involved on the seaward and landward slopes. Erosion on the seaward slope is caused by irregular breaking waves. Erosion on the landward slope is caused by intermittent wave overtopping of the levee whose crest elevation is normally designed to be higher than the design storm tide to avoid overflow. The similarity of the hydrodynamics involved in levee erosion and dune erosion is utilized herein to develop a numerical model for predicting the cross-shore and temporal variations of the erosion depth on the entire levee.

A levee erosion model is proposed by generalizing the work-based formula by Dean et al. (2010). The rate of work for levee erosion is expressed as the product of the vertical erosion rate and the resistance force of the grass and cohesive sediment. This rate of work is related to the energy dissipation rates due to wave breaking and bottom friction. The resistance force is assumed to decrease downward linearly in the turf zone with roots and be represented by the turf thickness and the surface and underneath resistance forces. The three parameters for the grass and soil characteristics are calibrated using available data.

LEVEE EROSION MODEL

The cross-shore model CSHORE for levee erosion (Kobayashi and Weitzner 2014) is explained for an emerged levee as depicted in Figure 1. Alongshore uniformity and normally incident waves are assumed. The cross-shore coordinate x is positive onshore with $x=0$ at the toe of the levee. The vertical coordinate z is positive upward with $z=0$ at the datum. The still water level (SWL) is located at the elevation of $z=S$ with S = storm tide. For comparisons with laboratory data with constant S, the datum is taken at SWL and $S=0$. The hydrodynamic model in CSHORE predicts the mean ($\overline{\eta}$ and $\overline{U}$) and standard deviation (σ_η and σ_U) of the free surface elevation η and depth-averaged cross-shore velocity U where the overbar denotes time averaging. The mean water level (MWL) is located at $z=\left(\overline{\eta}+S\right)$. The mean water depth $\overline{h}$ is given by $\overline{h}=\left(\overline{\eta}+S-z_b\right)$ with z_b = levee surface elevation varying with x. The intermittently wet and dry zone in CSHORE is assumed to occur landward of the still water shoreline located at $x=x_{\mathrm{SWL}}$. The wave overtopping rate q_o is

[1] Center for Applied Coastal Research, University of Delaware, nk@udel.edu
[2] HDR, Lafayette, Louisiana, Heather.Weitzner@hdrinc.com

estimated as the time-averaged volume flux at the most landward location x_c of the horizontal levee crest. The levee surface elevation z_b decreases slowly with time t because of erosion by irregular wave action. The eroded material is assumed to be transported out of the computation domain in the present levee erosion model.

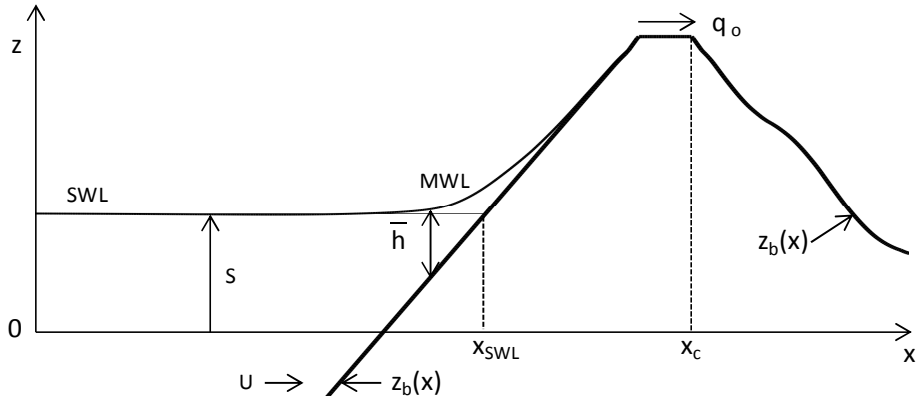

Figure 1. Definition sketch for levee erosion model.

The erosion model attempts to predict the temporal and cross-shore variations of the vertical erosion depth E defined as

$$E(t,x)=\left[z_b(t=0,x)-z_b(t,x)\right]\geq 0 \tag{1}$$

where the initial levee profile $z_b(x)$ at $t=0$ is input to the numerical model. The eroded levee profile $z_b(t,x)$ at given time $t>0$ can be predicted if $E=(t,x)$ is predictable. The resistance force of the turf per unit horizontal area is denoted as (ρR) with ρ = fluid density and R = resistance force divided by ρ with its unit being m^2/s^2. The rate of erosion work is expressed as the product of the resistance force and the vertical erosion rate

$$\rho R\frac{\partial E}{\partial t}=D \quad \text{with} \quad E=0 \ \text{ at } \ t=0 \tag{2}$$

where D = energy dissipation rate per unit horizontal area corresponding to the rate of erosion work. Subsequently, D is related to the rate of fluid energy dissipation. The vertical distribution of the turf resistance depends on the detailed root and soil structures. The simple distribution of R shown in Figure 2 is adopted and R is expressed as

$$R=R_0-(R_0-R_d)\frac{E}{d} \qquad \text{for} \ \ 0\leq E\leq d \tag{3}$$

$$R=R_d \qquad \text{for} \ \ d\leq E \tag{4}$$

where d = turf thickness; and R_0 and R_d = turf surface and underneath resistance parameters, respectively. The substrate resistance is assumed to be invariant vertically and represented by R_d. The grass cover is characterized by the three parameters d, R_0 and R_d which are allowed to vary spatially. Equation 2 can be integrated analytically for R given by Equations 3 and 4 for arbitrary D.

In the wet zone where water is present always, the dissipation rate D is assumed to be given by

$$D=\left(e_B D_B+e_f D_f\right)G_s(S_b) \quad ; \quad S_b=\frac{\partial z_b}{\partial x} \tag{5}$$

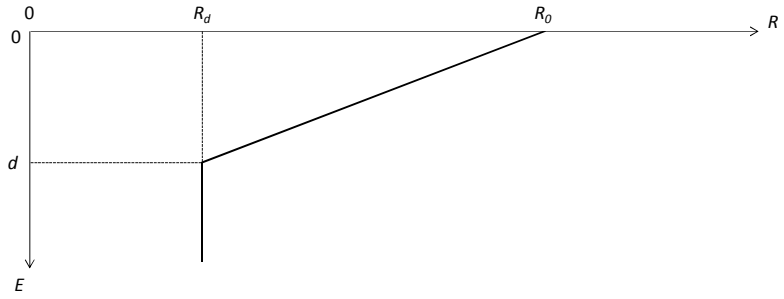

Figure 2. Resistance force parameter *R* as a function of vertical erosion depth *E*.

where D_B and D_f = energy dissipation rates per unit horizontal area due to wave breaking and bottom friction, respectively; e_B and e_f = efficiencies for D_B and D_f, respectively; and G_s = function of the bottom slope S_b with $G_s = 1.0$ for $S_b = 0$, introduced to increase erosion on the eroded steep slope of about $S_b = 1.0$. The efficiencies used for sand suspension are e_B = 0.005 and e_f = 0.01. The calibrated value of e_B for erosion of seaward levee slopes is e_B = 0.0002. Levee erosion by breaking waves is much less efficient than sand suspension by breaking waves. The value of e_f = 0.01 is adopted because the bottom friction acts more continuously than the intermittent breaking wave action. In the intermittently wet and dry zone $x \geq x_{\mathrm{SWL}}$ in Figure 1, no wave breaking is assumed to occur and D is given by

$$D = e_d D_f G_s(S_b) \quad \text{for} \quad x \geq x_{\mathrm{SWL}} \tag{6}$$

where the efficiency e_d is chosen so that the values of D given by Equations 5 and 6 are the same at $x = x_{\mathrm{SWL}}$ for the smooth transition between the two zones. The energy dissipation rate D_f due to bottom friction is expressed analytically, assuming the exponential probability distribution of the instantaneous water depth (Kobayashi and Weitzner 2014).

The computation procedure is as follows. The initial levee profile and the cross-shore variations of d, R_0 and R_d in Equations 3 and 4 are specified at time $t = 0$ before the time-marching computation. The time series of the still water level S and the spectral significant wave height H_{mo} and the peak period T_p at the seaward boundary $x = 0$ are also specified as input. The hydrodynamic model in CSHORE is used to compute the dissipation rate D given by Equations 5 and 6. The time step for the time-marching computation for large-scale and prototype levees is selected so that the computed erosion depth E does not increase more than 5 cm. The levee profile z_b at the next time level is obtained using Equation 1. This time-marching computation is repeated until the end of a levee erosion test. The computation time is of the order of 10^{-3} of the test duration. The computational efficiency is essential for the development of the levee erosion model which is empirical and requires the calibration of several parameters.

TURF FAILURE UNDER STEADY FLOW

The present levee erosion model is applicable to predict turf failure under steady flow on a gentle slope. The failure of a turf may be assumed to occur when the erosion depth E becomes equal to the turf thickness d which is taken as d = 0.1 m on the basis of the vertical decrease of the number of roots per unit surface area plotted by Hoffmans et al. (2008). Hewlett et al. (1987) plotted the limiting steady flow velocity as a function of its duration for turf failure. Their curves for the good, average, and poor grass covers are used to obtain $(R_0 + R_d) =$ 200 to 1200 m^2/s^2. The turf surface resistance parameter R_0 is expected to be much larger than the underneath resistance parameter R_d. The erosion

experiment of a seaward clay slope by Wolters et al. (2008) is used to calibrate $R_d = 10\,\mathrm{m}^2/s^2$ as will be shown later. In the following, a typical value of R_0 is taken as $R_0 = 1{,}000\ \mathrm{m}^2/\mathrm{s}^2$ for a good grass cover and $R_0 = 200\ \mathrm{m}^2/\mathrm{s}^2$ for a poor grass cover. These estimates may not be accurate but indicate the large variation of the turf and substrate resistance against erosion.

EROSION OF SEAWARD GRASSED SLOPE

Smith et al. (1994) excavated 16 blocks from a section of an existing sea levee in the Netherlands. The length, width, and thickness of each block were 2.5 m, 2.5 m, and 1.0 m, respectively. The blocks were transported to reconstruct the levee section in a large wave flume. The grass cover and clay substrate layer of 1-m thickness was placed on the seaward and landward slopes of 1/4 and 1/2.5, respectively. The grass cover was inspected in detail and found to be good. The width of the concrete crest was 2 m and the crest height was 7 m above the flume horizontal bottom. The levee erosion model is compared with the erosion tests 6 and 7. The water depth at the levee toe was 4.8 and 3.5 m for tests 6 and 7, respectively. The significant wave height H_s and the peak period T_p were 1.4 m and 4.7 s for test 6, respectively. For test 7, $H_s = 0.75$ m and $T_p = 3.4$ s. The test duration was 11 h for test 6 and 20 h for test 7. For the following computations, the spectral significant wave height H_{mo} is assumed to be the same as H_s and given by $H_{mo} = 4\sigma_\eta$. The good grass cover is represented by $d = 0.1\ m$, $R_0 = 1{,}000\ \mathrm{m}^2/\mathrm{s}^2$, and $R_d = 10\ \mathrm{m}^2/\mathrm{s}^2$ in Figure 2. The value of R_0 is increased to R_0 = 10,000 $\mathrm{m}^2/\mathrm{s}^2$ for the concrete sections of the constructed levee. These values should be regarded as order-of-magnitude estimates.

For test 6, the grass cover inspection and profile survey were performed every hour. The erosion depth E is computed and plotted in Figure 3 as a function of x at t = 1, 2, …, 11 h. The concrete sections correspond to the zones of x = 0 – 8 m and x = 28 – 30 m. The measured maximum erosion depth for test 6 was about 4 cm at t = 11 h in the zone of x = 15.8 – 17.5 m. The computed maximum erosion depth occurs closer to the still water shoreline located at x_{SWL} = 19.2 m. The computed erosion depth increases almost linearly with time t and is negligible on the landward slope (x > 30 m).

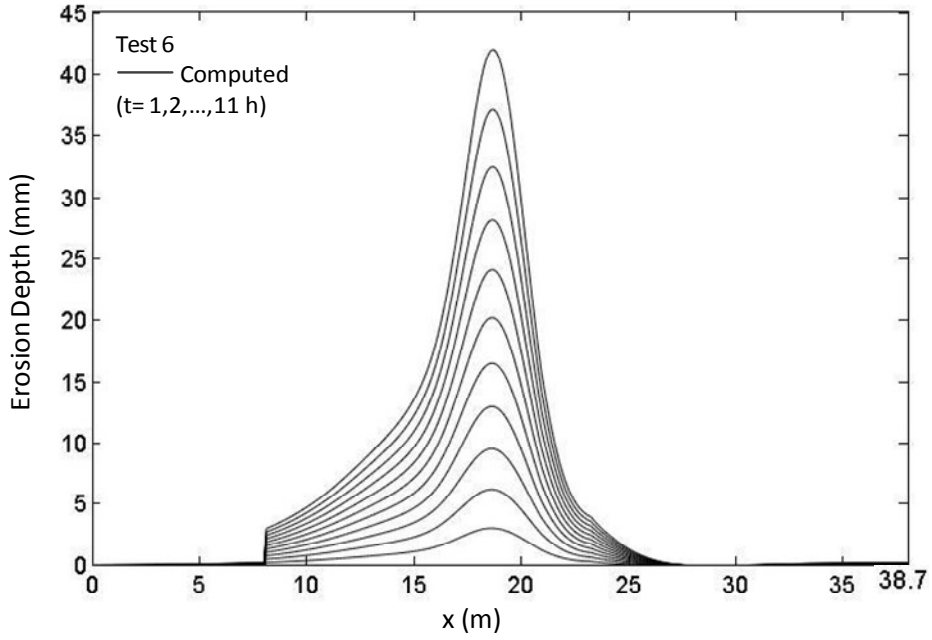

Figure 3. Computed erosion depth increase with time *t* for test 6 with H_s = 1.4 m

For test 7 with H_s = 0.75 m, the grass cover inspection and profile survey were performed every 4 hours. The computed maximum erosion depth at t = 20 h is less than 3 cm and occurs slightly below SWL (X_{SWL} = 14 m) as shown in Figure 4. The measured maximum erosion depth was about 2 cm at t = 20 h in the zone of x = 12.2 – 13.1 m. The landward limit of computed wave uprush is near x = 21 m well below the crest (x = 28 – 30 m).

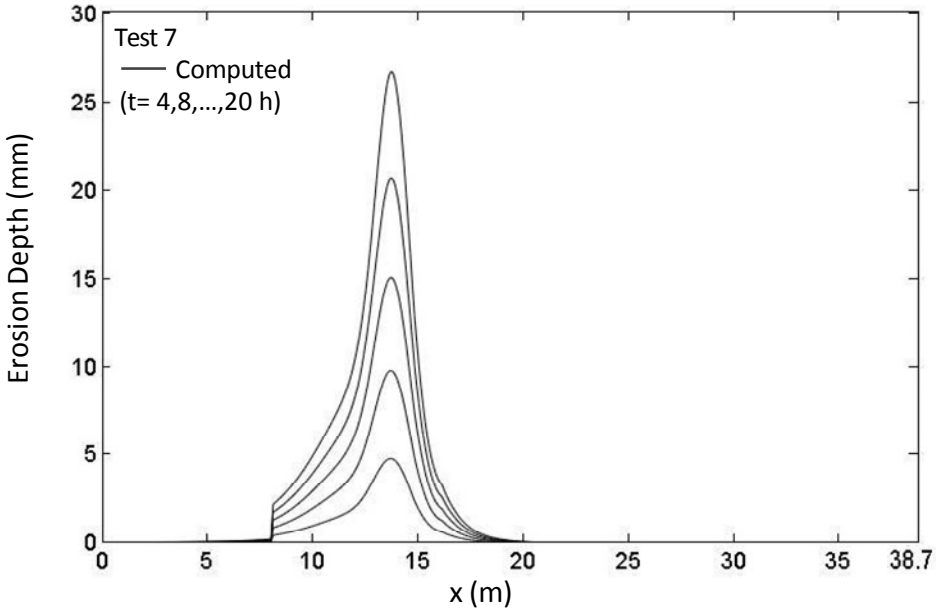

Figure 4. Computed erosion depth increase with time *t* for test 7 with H_s = 0.75 m

Smith et al. (1994) observed the development of a hole in test 6. The hole development was defined as the occurrence of local erosion progression through the root layer. The hole in test 6 occurred 1 m below SWL. The diameter and depth of the hole were 0.75 m and 0.12 m at t = 9 h, respectively, and increased to 1.0 m and 0.15 m at t = 11 hr. No hole was observed in test 7. The present levee erosion model based on the assumption of alongshore uniformity cannot predict the development of a three-dimensional hole. Erosion of a strip of a poor grass cover is analyzed instead. The strip of cross-shore width of 1.2 m is assumed to be located in the zone of 1.0 to 1.3 m below SWL. The surface resistance parameter R_0 is reduced to R_0 = 200 m^2/s^2 for the poor grass cover from R_0 = 1,000 m^2/s^2 for the good grass cover. Figure 5 shows the computed cross-shore variations of the erosion depth at t = 1, 2, … , 11 h for test 6 H where the letter H indicates a two-dimensional hole. The strip of the poor grass cover on the levee section in Figure 5 corresponds to the 1.2-m wide zone between the good grass cover indicated by short vertical lines. The erosion depth E for the good grass cover increases slowly with time t and is about 4 cm at t = 11 hr. The computed value of E for the poor grass cover becomes larger than the grass cover thickness of d = 10 cm at t = 9 hr and increases rapidly during t = 9 – 11 h. The computed erosion depth of E = 40 cm at t = 11 h is too large partly because the computed depth-averaged velocity U does not represent the reduced velocity inside the deep hole. The present levee erosion model does not predict the increase of the hole width after the hole development, probably because lateral erosion underneath the grass cover is not included in the model.

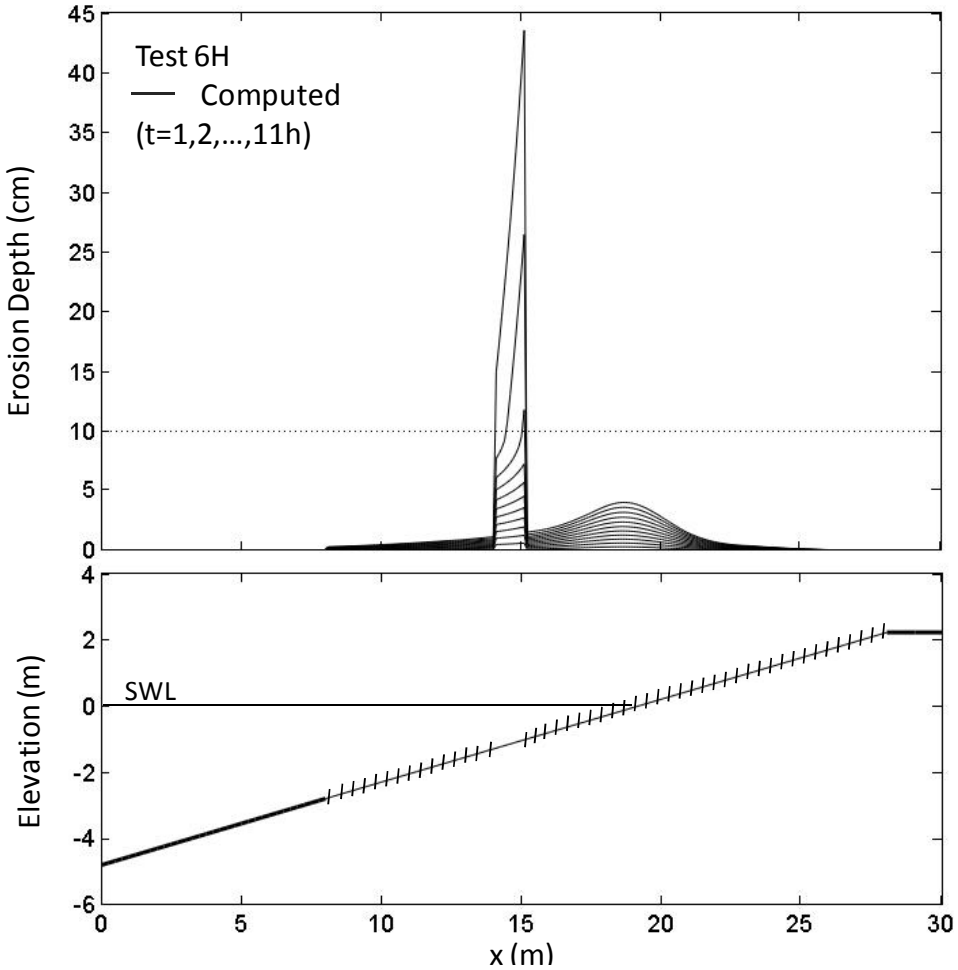

Figure 5. Computed erosion depth increase with time *t* for test 6 with poor grass patch and concrete sections ($x = 0 – 8$ m and $x = 28 – 30$ m)

Figure 6 shows the computed cross-shore variations of the erosion depth at $t =$ 4, 8, … , 20 h for test 7H with the 1.2-m wide strip of the poor grass cover. The erosion depth E increases with time but the hole development defined as $E > d$ = 10 cm through the poor grass cover does not occur because $E < 3$ cm at $t =$ 20 h. Figures 5 and 6 indicate that the turf resistance is as important as the wave forcing.

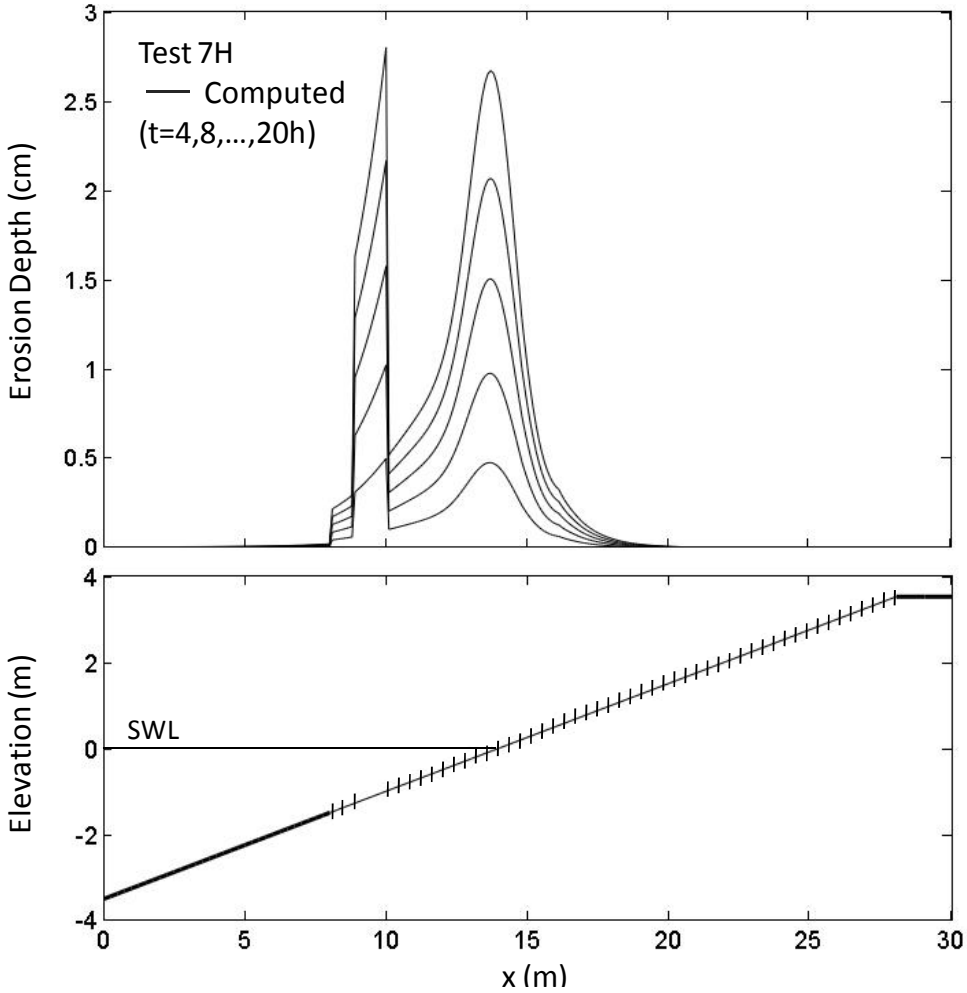

Figure 6. Computed erosion depth increase with time *t* for test 7H with poor grass patch

EROSION OF SEAWARD CLAY SLOPE

Wolters et al. (2008) removed the top layer of 1-m thickness from an old levee in the Netherlands and excavated 36 boulder clay blocks. The length, width, and height of each block were 1.8 m, 1.3 m and 1.6 m, respectively. The blocks were transported to construct a seaward clay slope of a levee in a large wave flume. The slope was 1/3 and the levee crest height was 8.3 m above the horizontal flume bottom. The water depth at the toe of the levee was 4.5 m. The maximum clay layer thickness was 3 m on the 1/3 slope. The clay layer extended from 1.6 m below SWL to 2.4 m above SWL. The zones below and above the clay layer were constructed of compacted clay and concrete. The boulder clay was structured clay with a network of cracks formed under the long-term weathering and erodes much faster than unstructured clay (Klein Breteler et al. 2012). For the following computation, $R_0 = 10{,}000\ \mathrm{m}^2/\mathrm{s}^2$ for the concrete and compacted clay is assumed to limit erosion to the boulder clay layer with $d = 0$ m and $R_d = 10\ \mathrm{m}^2/\mathrm{s}^2$. The wave conditions starting from $t = 0$ were varied in six steps at $t =$ 0.5, 1.31, 2.31, 3.55, 5.23, and 5.98 h (end of the last step). The spectral significant wave height H_{mo} was 1.12, 1.17, 1.51, 1.56, 1.58, and 1.57 m in the first to sixth steps. The corresponding peak period T_p was 4.97, 5.01, 5.73, 5.77, 5.72, and 5.98 s, respectively. The eroded clay profile was measured at the end of each step.

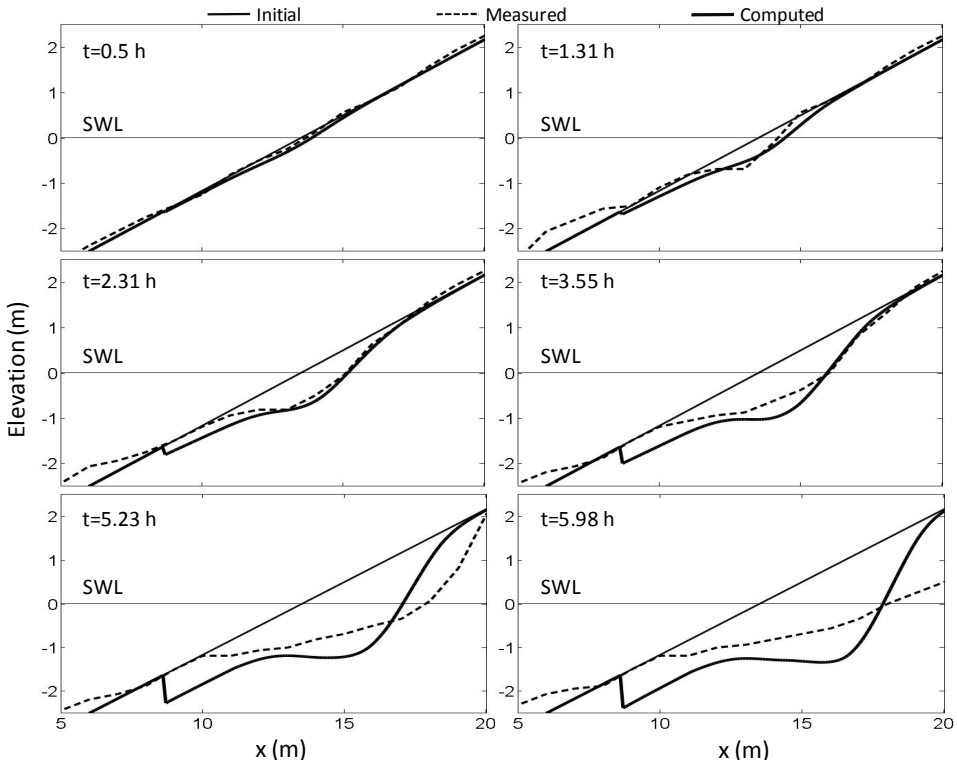

Figure 7. Measured and computed profile evolutions of seaward clay slope

Figure 7 compares the measured and computed profiles at $t =$ 0.5, 1.31, 2.31, 3.55, 5.23, and 5.98 h. The downward erosion is predicted well at $t =$ 0.5 and 1.31 h but overpredicted near $x =$ 8.7 m at $t =$ 2.31 to 5.98 h where the boundary between the boulder clay and compacted clay was located at $x =$ 8.7 m. The overprediction may be related partly to the deposition of the eroded clay in the zone of $x <$ 8.7 m where the eroded clay is assumed to be transported seaward of the levee toe at $x = 0$ in this levee erosion model. The computed erosion depth E is proportional to R_d^{-1} and can be decreased by reducing the breaking wave efficiency $e_B =$ 0.0002 in Equation 5. The adopted values of R_d and e_B are based on a number of computations made using the different combinations of R_d and e_B. The horizontal erosion of the eroded profile above SWL is predicted well at $t =$ 0.5 to 3.55 h but underpredicted at $t =$ 5.23 and 5.98 h. The boundary between the boulder clay and compacted clay was located at $x =$ 20.7 m and the measured profile close to this boundary was not presented by Wolters et al. (2008).

EROSION OF LANDWARD GRASSED SLOPE

Steendam et al. (2010) performed a number of tests on real levees to examine the behavior of the grass cover on the landward slope. These tests were conducted on the good grass cover. The numerical model is compared with test V1 because the cross section of the landward slope and crest of the Vecht levee for test V1 was presented by Steendam et al. (2010). The Wave Overtopping Simulator (van der Meer et al. 2010) simulates the overtopping wave volumes at the crest of an actual levee. The overtopping volumes of irregular waves were calculated for the specified significant wave height H_s and peak period T_p at the toe of a seaward slope of 1/4. The cross section of the levee in Figure 1 is based on that of test V1. The crest height of the levee above the datum $z = 0$ was 3.7 m and the crest width was 3m. The toe of the seaward 1/4 slope is assumed to be located at $z = -5$ m so that the

incident waves with $H_s = 2$ m and $T_p = 5.7$ s do not break seaward of the levee toe located at $x = 0$. The still water level S is chosen to produce the wave overtopping rate q_o on the crest specified for test V1. The hydrodynamic model in CSHORE for the fixed bottom is used to obtain the relation between S and q_o. The computed relation for $H_s = 2$ m and $T_p = 5.7$ s is shown in Figure 8. For $H_s = 2$ m, $q_o = 1 - 90$ ℓ/s/m for $S =$ (−1.2) – 2.0 m. The computed relation for $H_s =$ 1 m and $T_p =$ 4.0 s is also presented because van der Meer et al. (2010) examined the difference of individual wave overtopping volumes caused by the wave height difference for the same value of q_o. For $H_s =$ 1 m, $q_o = 1 - 90$ ℓ/s/m for $S =$ 1.8 – 3.4 m where $S =$ 3.7 m corresponds to the levee crest elevation. The rate q_o increases more rapidly with the increase of S for $H_s =$ 1 m than $H_s =$ 2 m.

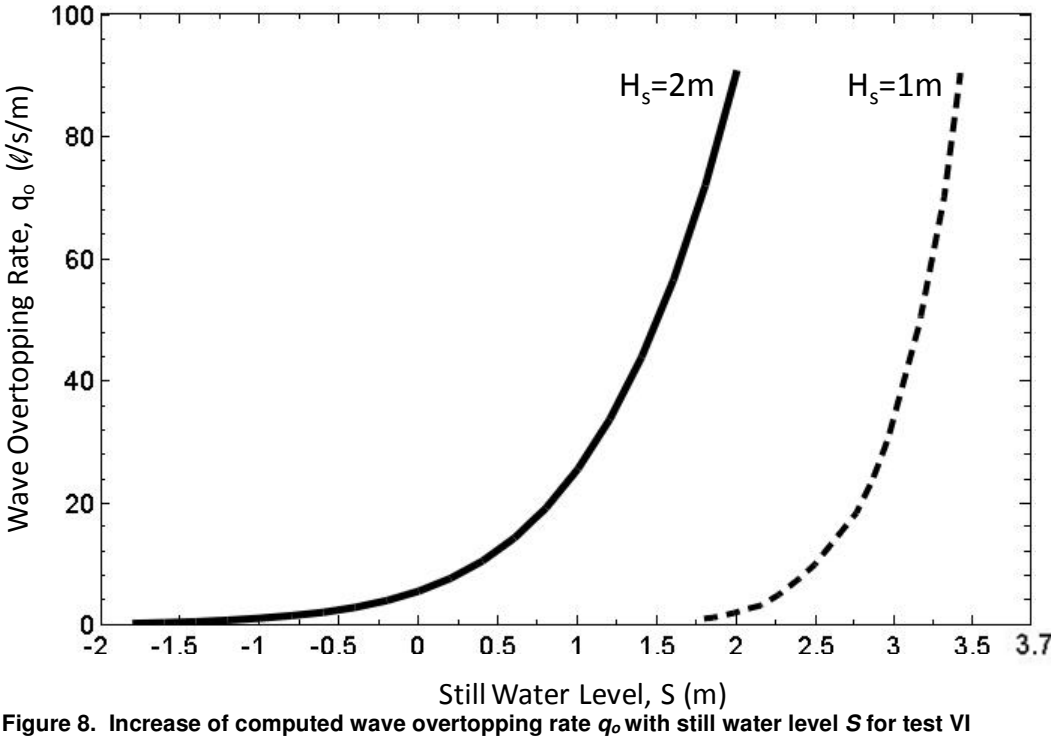

Figure 8. Increase of computed wave overtopping rate q_o with still water level S for test VI

The landward slope of test V1 is depicted in the bottom panel of Figure 9. A maintenance road was located in the middle of the slope. The grassed zones above and below the road are indicated by short vertical lines in Figure 9. The road consisted of bricks that allowed grass growth. The landward slope was subjected to the sequence of $q_o =$ 1, 10, 30 and 50 ℓ/s/m based on $H_s =$ 2 m. The duration of each value of q_o was 6 hours. Initial damage developed at the seaward edge of the maintenance road during $q_o =$ 1 ℓ/s/m. The initial damage progressed slowly during $q_o =$ 10 ℓ/s/m and evolved into two substantial holes undermining the road during $q_o =$ 30 ℓ/s/m. At the beginning of $q_o =$ 50 ℓ/s/m, some bricks were dislodged and some of the grass cover was eroded from the toe and berm in the zone of $x =$ 48 – 50 m in Figure 9.

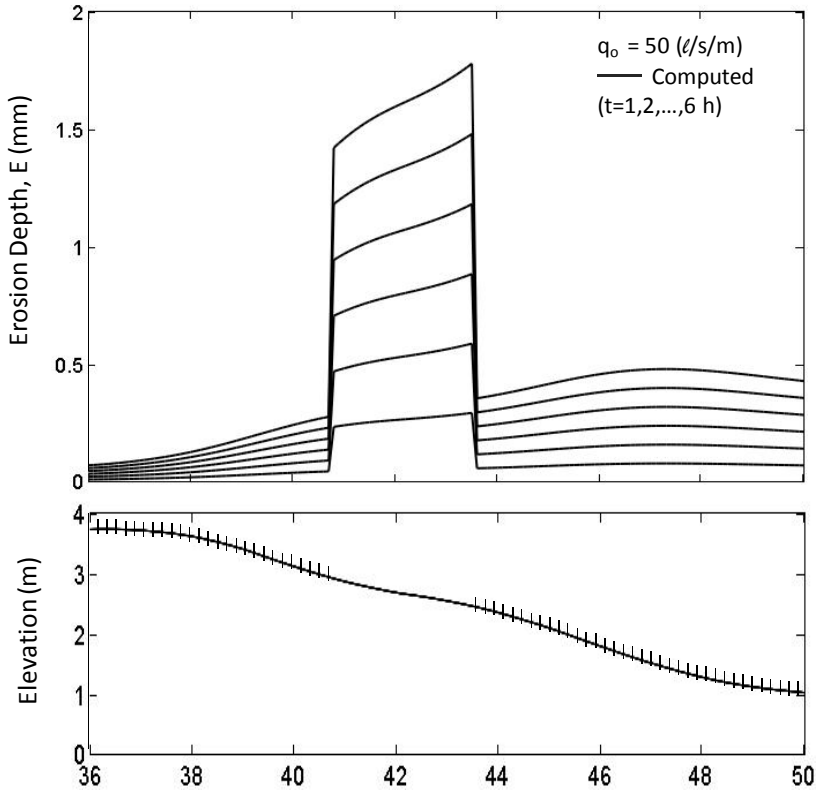

Figure 9. Computed erosion depth increase with time *t* for test VI with poor grass patch

The numerical model cannot simulate the observed damage progression in test V1 partly because local flow disturbance and damage initiation are not taken into account. Figure 9 shows the computed erosion depth E on the landward slope at $t =$ 1, 2, … , 6 h for $q_o =$ 50 ℓ/s/m where $E = 0$ at $t = 0$. The maintenance road is crudely represented as a strip of a poor grass cover with $R_0 =$ 200 m^2/s^2 where $R_0 =$ 1,000 m^2/s^2 for the good grass cover. The computed E of the poor grass cover at $t =$ 1 h is almost continuous with that of the good grass cover at $t =$ 5 h because E is approximately proportional to R_0^{-1} and t for the small erosion of 2 mm or less. The numerical model predicts the downward increase of E on the inclined slope but the predicted value of E is too small. The sensitivity of E to q_o in the range of $q_o =$ 1 – 90 ℓ/s/m is examined by computing the cross-shore variation of E on the landward slope of the same profile but covered with only the good grass cover. The maximum value of E occurs near the toe of the landward slope. The maximum erosion depth $E_{\max}$ increases with the increase of t and q_o but $E_{\max}$ is about 1 mm at $t =$ 6 h for $q_o =$ 90 ℓ/s/m. For the poor grass cover, $E_{\max}$ is about 5 mm at $t =$ 6 h for $q_o =$ 90 ℓ/s/m as shown in Figure 10. The computed $E_{\max}$ at $t =$ 1, 2, … , 6 h as a function of q_o for the landward clay slope with $R_0 = R_d = 10$ m^2/s^2 is about 10 cm at $t =$ 6 h for $q_o =$ 90 ℓ/s/m. The surface resistance parameter R_0 determines the degree of erosion on the landward slope. The wave overtopping rate q_o and duration t are also important but more predictable than the uncertain parameter R_0. The computed difference between $H_s =$ 2 m and 1 m is found to be small and q_o may be used to represent the erosion work by overtopping waves.

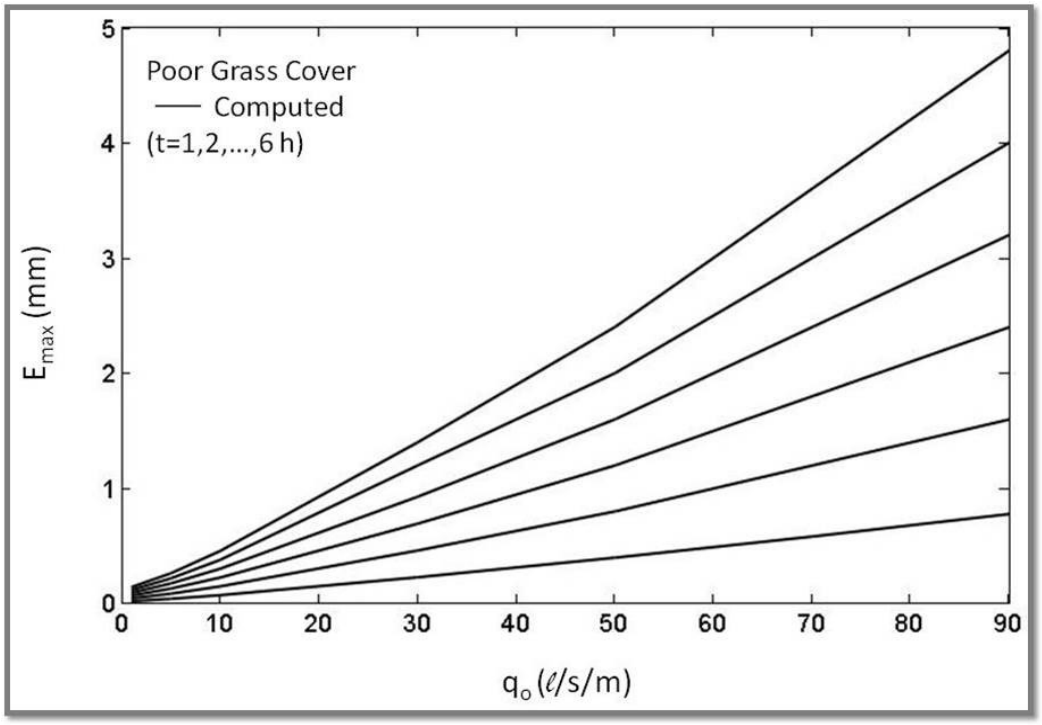

Figure 10. Computed maximum erosion depth E_{max} at slope transition of poor grass cover as a function of q_o and t

The computed results presented above are discussed in light of other available data. Thornton et al. (2011) examined resiliency of different landward slope surfaces using a large-scale wave overtopping test facility. The levee geometry consisted of a downward 1/3 slope with a height of 2.7 m that transitioned to a 3.6-m long berm on a 1/25 slope. This geometry is similar to that shown in Figure 9. Bermuda grass in planter trays was cultivated and well maintained for 6 months prior to testing. This grass cover with dense roots, ample thatching, and few imperfections suffered little damage under the 24-hour incremental increase of q_o up to 370 ℓ/s/m. The Bahia grass cover suffered little damage under the 17-hour incremental increase of q_o up to 279 ℓ/s/m. The grass cover model in Figure 2 with $R_0 =$ 200 – 1,000 m^2/s^2, $d =$0.1 m, and $R_d =$ 10 m^2/s^2 appears to correspond to the nearly perfect grass cover with few imperfections. The previously tested Bermuda grass went dormant during winter. The dormant Bermuda grass was tested in sequence of $q_o =$ 186,232 and 186 ℓ/s/m with a 1-hour interval. Minor erosion evolved into a 2.7-m long trench with a cross-flume width of 15-30 cm and a depth of 5-15 cm. This trench development is somewhat similar to the hole development discussed in relation to Figures 5 and 6. Thornton et al. (2011) also tested a bare clay surface. Significant soil loss occurred in one hour under $q_o =$ 9.3 ℓ/s/m. The bare clay test was continued under $q_o =$ 18.6 ℓ/s/m but suspended after 20 min because the clay slope failed catastrophically.

Steendam et al. (2012) conducted wave overtopping tests on a real levee with a poorly-maintained grass cover in contrast to the good grass cover tests by Steendam et al. (2010). The bad grass cover with holes made by moles had no resistance against overtopping waves. They concluded that a bad grass cover should be considered as an unprotected clay layer. The wave overtopping tests on real levees indicate the wide variations of grass covers. The simple grass cover model in Figure 2 may become more realistic if the spatial variations of R_0, R_d and d are known because damage tends to initiate from weak spots.

SUMMARY AND CONCLUSIONS

A levee erosion model is developed to predict the temporal and cross-shore variations of vertical erosion depth under irregular wave action. The product of the erosion rate and the turf resistance force is related to the wave energy dissipation rates due to wave breaking and bottom friction. The dissipation rates are computed using the hydrodynamic model in the cross-shore numerical model CSHORE. The turf resistance force is characterized by the turf thickness and the surface and underneath resistance parameters. The empirical parameters in the erosion model are calibrated using available data. The relation between the limiting velocity and steady flow duration is used to estimate the order of magnitude of the surface resistance parameter (200 – 1,200 m^2/s^2). Large-scale erosion tests for seaward grassed and clay slopes are used to estimate the underneath resistance parameter (10 m^2/s^2), the breaking wave efficiency (0.0002), and the limiting clay slope. Breaking waves are found to be much less efficient in eroding the cohesive levee than in suspending sand particles on beaches. The calibrated erosion model is shown to reproduce the erosion rate on the grassed slope and the eroded clay profile evolution. The levee erosion model is also compared with field tests for erosion on the landward slope caused by wave overtopping. The comparisons indicate the difficulty in reproducing the observed erosion initiation and progression partly because wave-induced flow in small water depth is affected by the surface irregularity and initial erosion tends to occur on weak spots.

ACKNOWLEDGMENTS

This study was partially supported by U.S. Army Corps of Engineers, Contract No. W911XK-13-P-0065 and the EU THESEUS Project.

REFERENCES

Dean, R.G., Rosati, J.D., Walton, T.L., and Edge, B.L. (2010). "Erosional equivalences of levees: Steady and intermittent wave overtopping." Ocean Eng., 37, 104-113.

Hewlett, H.W.M., Boorman, L.A., and Bramley, M.E. (1987). "Design of reinforced grass waterways." CIRIA Report 116, Construction and Industry Research and Information Association, London.

Hoffmans, G., Akkerman, G.J., Verheij, H., van Hoven, A., and van der Meer, J. (2008). "The erodibility of grassed inner levee slopes against wave overtopping." Proc. 31st Coastal Engineering Conf., World Scientific, Singapore, 3224-3236.

Klein Breteler, M., Bottema, M., Kruse, G.A.M., Mourik, G.C., and Capel, A. (2012). "Resilience of levees after initial damage by wave attack." Proc. 33rd Coastal Engineering Conf., Structures 36, 1-14. http://journals.tdl.org/ICCE/

Kobayashi, N., and Weitzner, H. (2014). "Erosion of a seaward dike slope by wave action." J. Waterway, Port, Coastal, Ocean Eng. (in press).

Smith, G.M., Seijffert, J.W.W., and van der Meer, J.W. (1994). "Erosion and overtopping of a grass levee: Large scale model tests." Proc. 24th Coastal Engineering Conf., ASCE, Reston, Va., 2639-2652.

Steendam, G.J., Provoost, Y., and van der Meer, J. (2012). "Destructive wave overtopping and wave run-up tests on grass covered slopes of real levees." Proc. 33rd Coastal Engineering Conf., Structures 64, 1-14. http://journals.tdl.org/ICCE/

Steendam, G.J., van der Meer, J., Hardeman, B., and van Hoven, A. (2010). "Destructive wave overtopping tests on grass covered landward slopes of levees and transitions to berms." Proc. 32nd Coastal Engineering Conf., Structures 8, 1-14. http://journals.tdl.org/ICCE/

Thornton, C., van der Meer, J., Scholl, B., Hughes, S., and Abt, S. (2011). "Testing levee slope resiliency at the new Colorado State University wave overtopping test facility." Proc. Coastal Structures 2011, World Scientific, Singapore, 167-178.

van der Meer, J., Hardeman, B., Steendam, G.J., Schüttrumpf, H., and Verheij, H. (2010). "Flow depths and velocities at crest and landward slope of a levee, in theory and with the wave overtopping simulator." Proc. 32nd Coastal Engineering Conf., Structures 10, 1-15. http://journals.tdl.org/ICCE/

Wolters, G., Nieuwenhuis, J.W., van der Meer, J., and Klein Breteler, M. (2008). "Large scale tests of boulder clay erosion at the Wieringermeer levee (Ijsselmeer)." Proc. 31st Coastal Engineering Conf., World Scientific, Singapore, 3263-3275.